Environmental Science & Technology

Article

pubs.acs.org/est

Evaluating the Transport of *Bacillus subtilis* Spores as a Potential Surrogate for *Cryptosporidium parvum* Oocysts

Scott A. Bradford,*[,†] Hyunjung Kim,[‡] Brendan Headd,[†] and Saeed Torkzaban[§]

[†]U.S. Salinity Laboratory USDA, ARS, 450 W. Big Springs Road, Riverside, California 92507-4617, United States

[‡]Department of Mineral Resources and Energy Engineering, Chonbuk National University, 664-14 Duckjin, Jeonju, Jeonbuk 561-756, Republic of Korea

[§]CSIRO Land and Water, Glen Osmond, SA 5064, Australia

Supporting Information

ABSTRACT: The U.S. Environmental Protection Agency has recommended the use of aerobic spores as an indicator for *Cryptosporidium* oocysts when determining groundwater under the direct influence of surface water. Surface properties, interaction energies, transport, retention, and release behavior of *B. subtilis* spores were measured over a range of physicochemical conditions, and compared with reported information for *C. parvum* oocysts. Interaction energy calculations predicted a much larger energy barrier and a shallower secondary minimum for spores than oocysts when the solution ionic strength (IS) equaled 0.1, 1, and 10 mM, and no energy barrier when the IS = 100 mM. Spores and oocysts exhibited similar trends of increasing retention with IS and decreasing Darcy water velocity (q_w), and the predicted setback distance to achieve a six log removal was always larger for spores than oocysts. However, low levels of observed spore and oocyst release significantly influenced the predicted setback distance, especially when the fraction of reversibly retained microbes (F_{rev}) was high. An estimate for F_{rev} was obtained from large release pulses of spore and oocyst when the IS was reduced to deionized water. The value of F_{rev} always increased with q_w, whereas an opposition trend for F_{rev} with IS was observed for spores (decreasing) and oocysts (increasing).

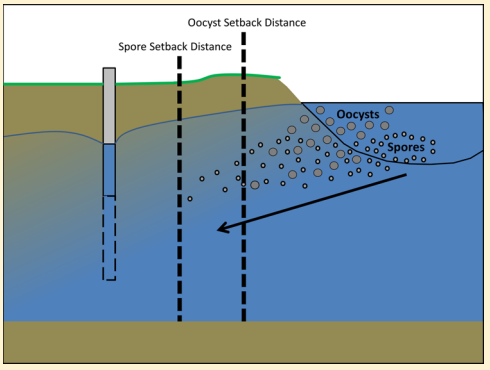

INTRODUCTION

Pathogenic microorganisms pose a risk to human health through recreational exposure in surface water, and contamination of drinking water and food supplies.[1,2] More than one billion people do not have access to clean drinking water and every year 2−5 million people die from waterborne diseases.[4,5] A number of rules and regulations have been put in place in the United States to protect drinking water supplies from microbial contamination. Beginning with the 1989 Surface Water Treatment Rule (SWTR) and continuing to the 2006 Long-term 2 Enhanced SWTR (LT2 Rule), the EPA has continually enhanced the requirements for public water systems to treat water sources to reduce the occurrence of disease causing microorganisms, including *Cryptosporidium*.[6] The Groundwater Rule relies on total coliform monitoring to establish groundwater sources that are vulnerable to microbial contamination.[7] Groundwater under the direct influence (GWUDI) of surface water is associated with greater risk of microbial contamination, and water utilities must take corrective action to reduce potential illness from exposure to microbial pathogens in their water sources.

The LT2 rule was designed to improve protection of drinking water supplies from *Cryptosporidium* oocysts.[8] *Cryptosporidium* is a protozoan pathogen that infects humans and animals. For example, *C. hominis* infects humans, whereas *C. parvum* is zoonotic.[9] Oocysts are shed into the environment through the feces of infected mammals and ingestion of as few as 10 oocysts can cause acute or persistent diarrhea in infected individuals that may be fatal in cancer or HIV patients, the very young, or the very old.[9,10] A number of waterborne disease outbreaks of Cryptosporidiosis have occurred in the United States and worldwide because of inadequate treatment of drinking water supplies.[11,12] *Cryptosporidium* oocysts are very highly resistant to chlorination during water treatment[13,14] and persistent in surface water and groundwater environments.[15,16] Consequently, treatment of drinking water supplies for *Cryptosporidium* oocysts frequently relies on engineered or natural filtration processes in soils, sediments, and aquifers.[8,17] However, accurate determination of the risk of *Cryptosporidium* in drinking water supplies is hampered by high costs and difficulty associated with producing and analyzing oocysts;[18] lack of reproducibility of assays for oocysts;[19] low oocyst concentrations in raw or treated waters;[20,21] and small sample volume and frequency.[22]

Received: October 28, 2015
Revised: December 22, 2015
Accepted: December 31, 2015
Published: December 31, 2015

DOI: 10.1021/acs.est.5b05296
Environ. Sci. Technol. 2016, 50, 1295−1303

Table 1. Interaction Energy Parameters for Aerobic Spores and Oocysts with Quartz Sand under Selected Solution IS Conditions and the Presence and Absence of Nanoscale Roughness

microbe	IS	h_r (nm)	f_r	ζ_m (mV)	ζ_s (mV)	$\Phi_{1\ min}$ (k_BT_k)	Φ_{max} (k_BT_k)	$\Phi_{2\ min}$ (k_BT_k)
spore	0.1	0	0	−47.5	−66.7	1096.8	1873.3	0.0
spore	0.1	25	0.05	−47.5	−66.7	1678.8	1700.3	0.0
spore	1	0	0	−51.2	−66.8	765.6	1405.6	0.0
spore	1	25	0.05	−51.2	−66.8	219.6	238.0	0.0
spore	10	0	0	−39.9	−61.8	788.6	1151.6	−0.6
spore	10	25	0.05	−39.9	−61.8	39.0	57.1	−0.3
spore	100	0	0	−15.6	−17.3	−415.1	NA	NA
spore	100	25	0.05	−15.6	−17.3	−21.8	NA	NA
oocyst	0.1	0	0	−19.8	−66.7	−12703.5	1800.8	0.0
oocyst	0.1	25	0.05	−19.8	−66.7	528.4	1789.3	0.0
oocyst	1	0	0	−5.9	−66.8	−15531.3	154.2	−0.3
oocyst	1	25	0.05	−5.9	−66.8	−678.5	38.4	−0.3
oocyst	10	0	0	−6.0	−61.8	−9304.1	107.1	−5.2
oocyst	10	25	0.05	−6.0	−61.8	−469.6	2.1	−2.1
oocyst	100	0	0	−6.6	−17.3	−2572.9	NA	NA
oocyst	100	25	0.05	−6.6	−17.3	−133.4	NA	NA

Given these limitations, a cost-effective and easily handled surrogate for *Cryptosporidium* oocysts is needed for determining GWUDI of surface water. Aerobic spores are commonly found in high concentrations in surface waters,[23] and have been investigated as a possible surrogate for *Cryptosporidium* oocyst transport and survival during filtration.[24−26] Headd and Bradford[27] summarize current knowledge about the survival, surface properties, and transport of aerobic spores and *Cryptosporidium* oocysts. In brief, oocysts are capable of surviving for months when exposed to a wide range of environmental conditions,[15] while aerobic spores can survive for many years in the environment.[28] Aerobic spores and oocysts also exhibit many similarities in surface properties, including: an isoelectric point below pH 3, neutral to strongly negative zeta potentials depending on the ionic strength and pH conditions, and glycoproteins on the exterior surface. Large variations in spore and oocyst hydrophobicity have been reported due to differences in the composition of the outer surface and age. Aerobic spores measure approximately 0.8 μm in width and 0.9−2 μm in length, and their density ranges from 1.29 to 1.335 g/cm^3. In contrast, oocysts tend to be larger in size (3.5−6 μm) and to have a lower density (1.045 g/cm^3). Difference in the size of aerobic spores and *Cryptosporidium* oocysts can influence mechanisms of retention and release. Larger microbes are known to be more susceptible to hydrodynamic forces, the secondary minimum, and microscopic roughness and pore structure. Conversely, smaller microbes are influenced to a greater extent by nanoscale roughness and chemical heterogeneity which locally reduce the energy barrier height to produce primary minimum interactions. Consequently, interactions are expected to be more reversible for oocysts than spores. The ability of aerobic spores to serve as a conservative surrogate for *Cryptosporidium* oocyst transport may therefore depend on the relative importance of site-specific physicochemical conditions. Based on available information, the U.S. Environmental Protection Agency researchers have recommended that determination of GWUDI be augmented with measurements of aerobic spore concentrations.[8,29] The implicit assumption is that aerobic spores are a conservative bioindicator of *Cryptosporidium* oocyst transport and survival. However, additional transport studies are needed to fully resolve this issue.

In this paper the surface properties, transport, retention, and release behavior of aerobic spores were assessed over a range in physicochemical conditions. These results are subsequently compared to similar data that have been published for *C. parvum* oocysts.[30] This comparison is designed to determine whether aerobic spores can serve as a conservative indicator for the transport of *C. parvum* oocysts in porous media. This information is expected to provide critical evidence for science-based decisions regarding procedures and protocols to determine GWUDI of surface water.

MATERIALS AND METHODS

Electrolyte Solutions and Porous Medium. Electrolyte solutions were prepared using deionized (DI) water (pH 5.6−5.8), and NaCl (0.1, 1, 10, and 100 mM) salt. Iota ultrapure quartz sand was employed as porous medium in the transport and release experiments discussed below. The sand was thoroughly rinsed with DI water to eliminate background fines from the sand before use. Zeta potentials for crushed ultrapure quartz sand in these electrolyte solutions were taken from the literature.[31,32] The median grain size of this sand was measured to be 238 μm (standard deviation of 124 μm) with a Horiba LA-930 analyzer.

***B. subtilis* ATCC 15476 Spore Preparation, Analysis, and Column Experiments.** *B. subtilis* ATCC 15476 was selected for transport studies based on published zeta potential and hydrophobicity measurements[33] which indicated that these spores might more closely resemble the surface properties of oocysts. *B. subtilis* ATCC 15476 was grown according to ATCC instructions. Section S1 in the Supporting Information (SI) contains details about the spore propagation and preparation. Based on microscopy, there was no aggregation among the spores or obvious signs of cellular debris from lysed cells. Concentrated spore suspension was diluted into a selected electrolyte solution to achieve an optical density at a wavelength of 600 nm (OD600) of approximately 0.2, which corresponds to an influent concentration (C_o) of about 2.5E7 spores/mL. Spore concentrations in the influent and column effluent were determined using Unico UV-2000 spectropho-

DOI: 10.1021/acs.est.5b05296
Environ. Sci. Technol. 2016, 50, 1295−1303

tometer readings at OD600 and a linear calibration curve. Spore size (~0.9 μm) and zeta potential in the influent suspension was determined using Horiba LA-930 and ZetaPals analyzers, respectively. The spore hydrophobicity was assessed by measuring the average air−water−solid contact angle on a bed of spores using a Tantec Contact Angle Meter. This bed was created by pipetting ~100 μL of concentrated spore suspension onto a microscope slide and allowing excess water to evaporate from the surface.

Glass chromatography columns (15 cm long and 4.8 cm inside diameter) were wet packed with the ultrapure quartz sand. The porosity, bulk density, and length for the packed column was determined to be about 0.46 cm^3 cm^{-3}, 1.43 g cm^{-3}, and 12.6 cm, respectively. A peristaltic pump was used to pump selected solutions upward through the vertically oriented columns at a steady Darcy velocity (q_w) of 0.2 or 0.5 cm min^{-1}. The column was equilibrated with a desired electrolyte solution for 10 pore volumes before initiating a transport experiment. Spore retention in the sand was achieved by pumping 2.8 pore volumes (PVs) through the column (Phase 1). Steady-state spore release was studied during Phase 2 by continued flushing of columns with microbe free solution having the same solution IS and q_w as Phase 1 for an additional 2 PVs (Phase 2). Transient spore release was studied during Phase 3 by systematically changing the solution IS to DI water for 4 PVs, while keeping q_w the same. Spore release was initiated during Phase 3 by alteration of the interaction energy profile (Table 1). A 12 h flow interruption was initiated during the middle of Phase 3 to allow sufficient time for diffusive release to occur from a primary minimum and/or microscopic roughness location in the presence of DI water. Effluent samples during Phases 1−3 were continuously collected at selected intervals using a fraction collector. The effluent samples were then analyzed for spores using the spectrophotometer as described above. All experiments were replicated at room temperature (~25 °C) and exhibited good reproducibility.

C. parvum Oocyst Preparation, Analysis, and Column Experiments. A detailed discussion of the preparation, analysis, and column experiments for *C. parvum* oocysts was presented in Kim et al.[30] A summary of this information is provided in section S2 of the SI.

Interaction Energy Calculations. The total interaction energy (Φ) of spores and oocysts upon approach to the ultrapure quartz sand under the various solution chemistries was calculated using extended Derjaguin−Landau−Verwey−Overbeek (XDLVO) theory and a sphere-plate assumption.[34,35] Electrostatic double layer interactions were quantified with the expression of Hogg et al.,[36] using zeta potentials in place of surface potentials.[37] The retarded London-van der Waals attractive interaction force was determined with the expression of Gregory,[38] using a Hamaker constant of 6.5×10^{-21} J for spores and oocysts.[39] Born repulsion was accounted for with the expression of Ruckenstein and Prieve[40] in which the collision diameter was set equal to 0.26 nm. XDLVO calculations were conducted for (i) geometrically smooth surfaces; and (ii) a uniform distribution of nanoscale roughness of height (h_r) and density (f_r) on the grain surface equal to 25 nm and 0.05, respectively. These roughness parameters have previously been shown to have a large influence on the interaction energy profile.[41] Details of the XDLVO calculations are provided in section S3 of the SI.

Mathematical Model. The HYDRUS-1D computer code[42] was used to simulate the breakthrough curves of aerobic spores and *Cryptosporidium* oocysts[30] under various physicochemical conditions. The two-site retention model allows for different fractions of reversible (F_{rev}) and irreversible ($F_{irrev} = 1 - F_{rev}$) microbe retention. The values of F_{rev} and F_{irrev} can be explicitly incorporated into the model as shown below. In this case, the aqueous and solid phase mass balance equations for the microbes are given as

$$\frac{\partial \theta_w C}{\partial t} = \frac{\partial}{\partial z}\left(\theta_w D \frac{\partial C}{\partial z}\right) - \frac{\partial q_w C}{\partial z} - \theta_w(\mu_1 + F_{rev}k_{sw} + F_{irrev}k_{sw})C + \rho_b k_{rs} S_1 \quad (1)$$

$$\frac{\partial(\rho_b S_1)}{\partial t} = \theta_w F_{rev} k_{sw} C - \rho_b(\mu_s + k_{rs})S_1 \quad (2)$$

where θ_w [−] is the volumetric water content, C [N_c L^{-3}, L and N_c denote the units of length and the number of microbes, respectively] is the aqueous phase microbe concentration, t is time [T, T denotes time units], z [L] is the distance from the column inlet, D [L^2T^{-1}] is the hydrodynamic dispersion coefficient, k_{sw} [T^{-1}] is the first-order retention coefficient, k_{rs} [T^{-1}] is the first-order release coefficient, ρ_b [M L^{-3}, M denote units of mass] is the soil bulk density, S_1 [N_c M^{-1}] is the solid phase microbe concentrations for reversible site 1, and μ_l [T^{-1}] and μ_s [T^{-1}] are the first-order microbial decay coefficients in the liquid and solid phases, respectively. This model accounts for dispersive and advective fluxes, liquid and solid decay, and reversible and irreversible microbial retention on the solid phase. However, unique estimates for F_{rev} can only be determined from release data that recovers a significant fraction of S_1. Blocking may also be easily incorporated into the eqs 1 and 2, but it was neglected because preliminary simulations revealed that spore and oocyst data typically did not exhibit blocking behavior; for example, a large standard error for the fitted maximum solid phase microbe concentration (with exception of oocysts data at IS = 0.1 mM). This assumption is further justified when considering low inputs of C_o in the environment.

Values of q_w and θ_w that were employed in the simulations were determined directly from experimental measurements. Conversely, the dispersivity value that was used in simulations was determined by inverse optimization to the breakthrough curve at the lowest IS = 0.1 mM which had minimal retention and behaved similar to a conservative tracer. This value of dispersivity (0.075 and 0.07 cm when q_w was 0.2 and 0.5 cm min^{-1}, respectively) was used for subsequent simulations at higher IS levels. Each microbial data set was analyzed using the fully reversible retention model by setting F_{rev} = 1, and neglected decay (μ_l = 0 and μ_s = 0). In this case, values of k_{sw} and k_{rs} were determined by inverse optimization to the breakthrough curve data.

The setback distance to achieve a desired reduction in C_o was calculated from the steady-state analytic solution of eqs 1 and 2 when D = 0 as

$$z = -\frac{q_w}{\theta_w\left(\mu_l + F_{irrev}k_{sw} + \mu_s \frac{F_{rev}k_{sw}}{(k_{rs}+\mu_s)}\right)} \ln\left(\frac{C}{C_o}\right) \quad (3)$$

Section S4 of the SI provides details on this derivation.

DOI: 10.1021/acs.est.5b05296
Environ. Sci. Technol. 2016, 50, 1295−1303

Table 2. Experimental (Porosity, ε; and Darcy Velocity, q_w) and Model (Retention Coefficient, k_{sw}; and Release Coefficient, k_{rs}) Parameters for the Aerobic Spore and Oocyst Column Experiments Conducted under Various Physicochemical Conditions[a]

Microbe	IS mM	ε	q_w (cm min-1)	k_{sw} (min^{-1})	k_{rs} (min^{-1})	R^2	M_{eff}[b]	F_{rev}[b]	Setback (m)
spores	0.1	0.46	0.2	2.7×10^{-3}	5.8×10^{-3}	1.00	0.94	0.50	22.2
spores	1	0.47	0.2	6.2×10^{-2}	1.1×10^{-4}	0.97	0.17	0.42	1.0
spores	10	0.46	0.2	1.1×10^{-1}	4.0×10^{-8}	0.82	0.04	0.34	0.5
spores	100	0.45	0.2	2.0×10^{-1}	3.1×10^{-6}	0.11	0.00	0.25	0.3
spores	0.1	0.45	0.5	9.9×10^{-3}	1.1×10^{-2}	0.97	0.94	1.00	15.5
spores	1	0.46	0.5	8.2×10^{-2}	2.6×10^{-3}	0.97	0.41	0.80	1.8
spores	10	0.46	0.5	3.2×10^{-1}	4.0×10^{-3}	0.77	0.04	0.42	0.5
spores	100	0.47	0.5	4.5×10^{-1}	3.2×10^{-3}	0.11	0.01	0.30	0.3
oocysts	0.1	0.47	0.2	3.6×10^{-2}	3.1×10^{-3}	0.95	0.51	NM	1.4
oocysts	1	0.47	0.2	5.5×10^{-2}	1.1×10^{-3}	0.99	0.26	0.58	0.9
oocysts	100	0.47	0.2	2.0×10^{-1}	1.7×10^{-3}	0.02	0.01	NM	0.2
oocysts	0.1	0.47	0.5	5.6×10^{-2}	3.6×10^{-3}	0.92	0.69	NM	2.6
oocysts	1	0.47	0.5	1.1×10^{-1}	1.9×10^{-3}	0.93	0.40	NM	1.3
oocysts	100	0.47	0.5	5.5×10^{-1}	3.6×10^{-3}	0.22	0.01	NM	0.3

[a]Also shown are the Pearson's correlation coefficient (R^2), the effluent mass balance (M_{eff}) for Phases 1 and 2, the reversible fraction of the retained microbes (F_{rev}) for Phase 3, and the calculated setback distance to achieve a six log reduction in the influent concentration. NM, denotes not measured. [b]See Table S1 for full mass balance details.

RESULTS AND DISCUSSION

Surface and Interaction Properties. Table 1 presents a summary of zeta potential and calculated interaction parameters for *B. subtilis* spores and *C. parvum* oocysts with ultrapure quartz sand under selected IS (0.1., 1, 10, and 100 mM) conditions. Section S5 of the SI contains a discussion of the zeta potential information, along with a plot of spore, oocyst, and quartz zeta potentials as a function of IS (Figure S1). Interaction energy calculations for smooth surfaces indicate the presence of no or a shallow secondary minimum for spores and oocysts when the IS was 1 and 10 mM, with a greater depth of the secondary minimum occurring at the higher IS (10 mM) and for the larger microbe (oocyst). An insurmountable energy barrier to attachment in the primary minimum was predicted for spores and oocysts at ionic strengths of 0.1, 1, and 10 mM (all >107 kT). No energy barrier was predicted at IS = 100 mM for both spores and oocysts, but the depth of the primary minimum was finite because of Born repulsion.

An illustration of the potential influence of nanoscale roughness on the interaction energy parameter for spores and oocysts is also presented in Table 1 when h_r = 25 nm and f_r = 0.05. In comparison to the perfectly smooth grains, nanoscale roughness decreased and sometimes eliminated the energy barrier to the primary minimum (e.g., oocysts at IS = 10 mM), and reduced the depth of the primary and secondary minimum. However, these effects of nanoscale roughness were much more pronounced on oocysts than spores because of their higher (less negative) zeta potentials (Figure S1) and lower energy barriers (Table 1). It is interesting to note that the depth of the primary minimum was a strong function of solution IS, and that increasing the IS actually reduced the magnitude of the primary minimum for oocysts. The combined influence of nanoscale roughness and Born repulsion can produce a shallow primary minimum from which colloids are susceptible to diffusive and/or hydrodynamic removal.[41,43−45] Diminished retention of oocysts and other microbes at higher IS has been attributed to electrosteric repulsion.[30,32,39,46−48] Table 1 suggests that consideration of the influence of nanoscale roughness on interaction energy profiles provides an alternative explanation. The potential effects of nanoscale chemical heterogeneity on interaction energies were not considered in this work, but this topic was addressed in a recent review article.[27]

Hydrophobicity is a second surface property of spores and oocysts that can potentially influence surface interactions. The contact angle for *B. subtilis* aerobic spores was strongly hydrophilic (~20°). Similarly, oocysts have also been reported to be hydrophilic.[39,48]

Transport and Retention. This section discusses the transport and retention behavior of aerobic spores and oocysts under various physicochemical conditions. Kim et al.[30] previously reported on the oocyst data. The oocyst data was modeled, further analyzed, and compared with the aerobic spore data in this work. Table 2 provides a summary of mass balance information for spore and oocyst experiments; full mass balance details are provided in Table S1. Table 2 also presents a summary of the fitted model parameters (k_{sw} and k_{rs}) when F_{rev} = 1, and the Pearson's correlation coefficient (R^2). The model provided a good description of the measured breakthrough curves (R^2 > 0.92) when effluent mass balance (M_{eff}) was greater than around 0.04 (Table 2). The value of R^2 was considerable lower and standard error on k_{sw} and k_{rs} (SI Table S2) were larger when C/C_o approached the analytic detection limit (<2% of C_o).

Figure 1 presents measured and simulated breakthrough curves for aerobic spores when the solution IS was equal to 0.1, 1, 10, and 100 mM NaCl and q_w was 0.2 (Figure 1a) and 0.5 (Figure 1b) cm min^{-1}. In general, spore transport and retention were very sensitive to the solution IS. At an IS = 0.1 mM there was very little retention at either Darcy velocity (M_{eff} = 0.94). This result was consistent with the interaction energy calculations that predict no secondary minimum and a large energy barrier to the primary minimum (Table 1). In this case, the small amounts of spore retention (~6%) were likely due to the coupled influence of nanoscale roughness and chemical heterogeneity, and microscopic roughness (and/or grain−grain contacts). Small amounts of nanoscale roughness on the grain (Table 1) or microbe (not considered in our XDLVO calculations) can locally reduce or eliminate the energy barrier to the primary minimum.[44,49] Chemical heterogeneity on the grain or microbe that is equal to or greater than the size of the

DOI: 10.1021/acs.est.5b05296
Environ. Sci. Technol. 2016, 50, 1295−1303

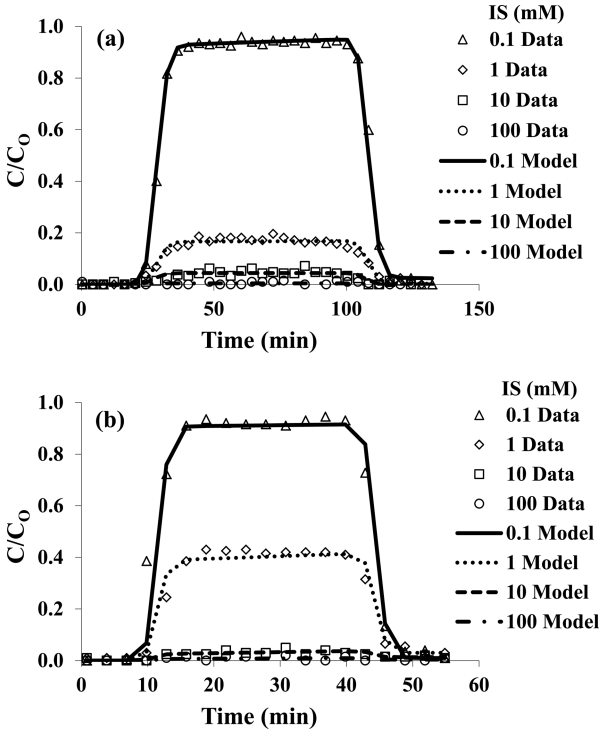

Figure 1. Measured and simulated breakthrough curves for aerobic spores when the Darcy velocity (q_w) was 0.2 (Figure 1a) and 0.5 (Figure 1b) cm min^{-1} and the IS was equal to 0.1, 1, 10, and 100 mM NaCl.

electrostatic zone of influence may also produce localized regions that are favorable for spore retention.[49,50] Microscopic roughness on grain surfaces enhances microbe retention by reducing the lever arm associated with the applied hydrodynamic torque and increasing the lever arm for resisting adhesive torque.[51,52] Microscopic roughness has been demonstrated to control colloid retention at low solution IS and higher q_w, whereas nanoscale roughness and chemical heterogeneity dominate retention under the opposite conditions.[45] The role of microscopic roughness and grain−grain contacts on oocysts retention has been previously demonstrated.[30,53−55]

A small increase in the solution IS from 0.1 to 1 mM produced a dramatic increase in spore retention from M_{soil} = 0.06 to 0.59−0.83 (Table S1), respectively. This observation likely reflects the increasing influence of nanoscale roughness and chemical heterogeneity on retention at higher IS.[45] When the solution IS = 1 mM, nearly 83% of the spores were retained at the lower q_w = 0.2 cm min^{-1}, whereas only 59% were retained at q_w = 0.5 cm min^{-1}. A corresponding increase in k_{sw} from 0.062 to 0.082 min^{-1} was observed as q_w increased from 0.2 to 0.5 cm min^{-1} (Table 2). Similarly, filtration theory predicts an increase in k_{sw} of 23% due to differences in the spore mass transfer rate to the grain surface when q_w increases from 0.2 to 0.5 cm min^{-1};[56,57] for example, favorable (all collisions lead to immobilization) values of k_{sw} (k_{fav}) for spores were predicted to be 0.17 and 0.21 min^{-1} when q_w = 0.2 and 0.5 cm min^{-1}, respectively. At IS of 10 and 100 mM nearly all of the spores were retained at both velocities (≥96%). In contrast, the interaction energy calculations on nanoscale rough and especially smooth surfaces predict only significant adhesive forces for the IS = 100 mM condition (Table 1). As for the IS = 1 mM data, these observations likely reflect an increasing influence of nanoscale roughness and chemical heterogeneity on retention with increasing IS.

Similar to spores, the amount of oocyst retention increased with IS (SI Table S1 and Table 2). Values of k_{sw} also increased with q_w for spores and oocysts (Table 2). These observations suggest that spores and oocysts respond in a similar manner to physicochemical conditions. An explanation for the dependence of oocyst retention on IS and q_w was previously provided by Kim et al.[30] In brief, these authors reported that oocyst retention was controlled by low velocity regions near grain−grain contacts, weak attractive interactions from the secondary minimum, and/or nanoscale roughness and chemical heterogeneity when the IS = 0.1 and 1 mM, and electrosteric repulsion when the IS = 100 mM. Alternatively, Table 1 indicates that nanoscale roughness may have contributed to lower than expected values of k_{sw} for oocysts when the IS = 100 mM.

Information presented in SI Table S1 and Table 2 can be used to compare the transport and retention behavior of aerobic spores with oocysts. Significantly, the value of k_{sw} was always larger for oocysts than spores for the same physicochemical conditions. Assuming negligible microbe release (F_{irrev} = 1), higher values of k_{sw} produced a smaller setback distance for oocysts than spores to achieve a 6 log reduction in C_o (eq 3 and Table 2). This indicates that spores can serve as a conservative surrogate for oocyst transport and retention. The calculated setback distance ranged from 0.3 to 22.3 m depending on the physicochemical conditions, and larger setback distances were always associated with lower IS. The deviation between spore and oocyst setbacks also increased at lower IS, and spores likely provided an overly conservative estimate for the oocyst setback distance when IS = 0.1 mM. The dependency of the setback distance on q_w was more complicated than IS. At the lowest IS levels of 0.1 and 1 mM with the greatest transport potential, larger setback distances tended to be associated with higher q_w. The one exception was for spores at IS = 0.1 mM. In this case, little retention occurred at both q_w.

Differences in k_{sw} for spores and oocysts under the same physicochemical conditions can be explained in part by the mass transfer rate. Values of k_{fav} for spores and oocysts were determined using filtration theory[56] and a correlation equation for the single collector efficiency[57] to be 0.17 and 0.18 min^{-1}, respectively, when q_w = 0.2 cm min^{-1}. A similar increase in k_{fav} (0.21 min^{-1} for spores and 0.28 min^{-1} for oocysts) was predicted when q_w = 0.5 cm min^{-1}. Hence, mass transfer considerations indicate that spores will act as a conservative surrogate for oocyst transport and retention behavior. A similar finding was reported by Headd and Bradford[27] over a range in sand grain sizes and q_w. Nearly complete retention occurred for spores when the IS = 10 and 100 mM, and for oocysts when the IS = 100 mM (Table 2). In this case, differences in mass transfer are expected to control k_{sw} values. However, experimental values of k_{sw} at IS levels of 0.1 and 1 mM (Table 2) were much lower than filtration theory predictions because of highly unfavorable conditions for microbe retention (Table 1). The sticking efficiency (k_{sw}/k_{fav}) for spores (α_s) was calculated to be much lower than for oocysts (α_o) when the IS = 0.1 mM because of their larger energy barrier (Table 1) and decreasing influence of microscope roughness for smaller sized colloids;[45] for example, α_s = 0.02 and α_o = 0.21 at q_w = 0.2 cm min^{-1}, and α_s = 0.05 and α_o = 0.20 at q_w = 0.5 cm min^{-1}. In contrast, values of α_s and α_o were quite similar when the IS = 1

DOI: 10.1021/acs.est.5b05296
Environ. Sci. Technol. 2016, 50, 1295−1303

mM, presumably because of the increasing influence of nanoscale roughness and chemical heterogeneity on retention, especially for smaller colloids;[45] for example, α_s = 0.37 and α_o = 0.32 at q_w = 0.2 cm min^{-1}, and α_s = 0.39 and α_o = 0.40 at q_w = 0.5 cm min^{-1}. Hence, calculated sticking efficiencies under low IS conditions also indicated that spores will serve as a conservative indicator of oocyst transport and retention.

Steady-State Release. The above information indicates that aerobic spores will be a conservative surrogate for oocyst transport and retention over a range in physicochemical conditions. However, this analysis neglected the potential influence of release on microbial fate. Low concentration levels of spore and oocyst release were observed in column experiments under constant physicochemical conditions. The microbial release rates are given by k_{rs} in Table 2. Systematic changes in k_{rs} with solution IS, q_w, and microbe type were not observed, possibly because the low concentration levels approached the analytic detection limit.

The calculated setback distances (eq 3) in Table 2 neglected release. Although the microbial release rates were small, they will strongly influence the needed setback distance to ensure a 6 log removal. Figure 2 presents a semilog plot of predicted

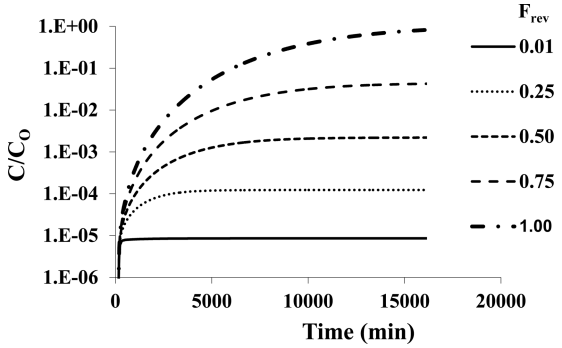

Figure 2. Predicted values of oocyst C/C_o as a function of time at a distance of 1 m when the IS = 1 mM and q_w = 0.2 cm min^{-1}. The predictions were obtained using model parameters shown in Table 2 assuming that the reversible fraction (F_{rev}) of retained oocyst was 0.01, 0.25, 0.50, 0.75, and 1.00 and a constant input concentration value of C_o.

relative effluent concentrations (C/C_o) for oocysts at a distance of 1 m when the solution IS = 1 mM and q_w = 0.2 cm min^{-1}. All simulations had the same overall k_{sw} = 0.055 min^{-1}, but different values of F_{rev} = 0.01, 0.25, 0.5, 0.75, and 1. Separate values of k_{rs} had to be fitted to the oocyst breakthrough curve for each F_{rev} condition because of differences in S_1. Fitted values of k_{rs} equaled 1.1 × 10^{-1}, 7.0 × 10^{-3}, 2.5 × 10^{-3}, 1.6 × 10^{-3}, and 1.1 × 10^{-3} min^{-1} when F_{rev} = 0.01, 0.25, 0.5, 0.75, and 1, respectively, and provided a good description of the oocyst retention and release when $F_{rev} \geq 0.25$. Release was underestimated in the experiment when F_{rev} = 0.01, even though a very large value of k_{rs} = 1.1 × 10^{-1} min^{-1} was employed, because S_1 was too small.

Figure 2 indicates that very little oocyst breakthrough was predicted at 1 m when F_{rev} = 0.01 because almost all of the oocysts were irreversibly retained. This result was consistent with the calculated setback distance (eq [3]) of 0.9 m in Table 2. However, as F_{rev} increased from 0.01 to 1 the peak value of C/C_o dramatically increased from 8.6 × 10^{-6} to 1. Hence, the assumption of a 6 log removal for oocysts at a distance of 1 m from the source was not valid when $F_{rev} \geq 0.01$. Persistent low concentration tailing for hundreds to thousands of pore volumes has been observed following recovery of the oocyst breakthrough curve.[58,59] Harter et al.[58] reported that up to half of the initially retained oocysts appeared to be reversible. In addition, multiple sites for kinetic retention and release have been required to describe oocyst transport.[55,60] These observations suggest that F_{rev} is a critical factor in determining the appropriate setback distance.

It should be acknowledged the above setback distance analysis neglected the influence of microbial decay, which may also contribute to the setback distance. Equation 3 indicates that increasing μ_l and μ_s will produce a decrease in the setback distance. Review of the literature indicates that spores are a conservative surrogate of oocyst decay;[27] for example, μ_l and μ_s are expected to be smaller for spores than oocysts. In this case, eq 3 and k_{sw} values in Table 2 indicate that spores will be a conservative indicator of oocyst setback distances provided that F_{rev} values are similar.

Transient Release. Transient solution chemistry and water flow conditions may also have a strong impact on microbial release processes that influence setback distances. Figure 3

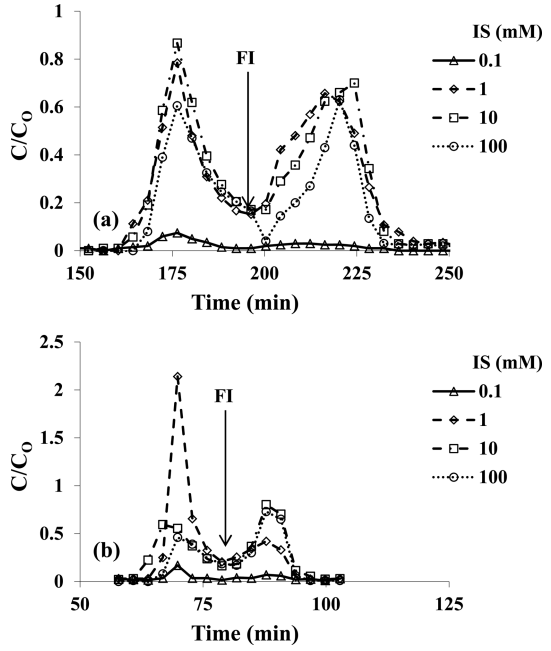

Figure 3. Measured release curves for aerobic spores when the Darcy velocity (q_w) was 0.2 (Figure 3a) and 0.5 (Figure 3b) cm min^{-1} and the IS was reduced from 0.1, 1, 10, and 100 mM NaCl to DI water. A 12 h flow interruption (FI) was initiated at the indicated time that was followed by continued flushing of DI water at the same flow rate.

presents measured release curves for aerobic spores when the IS was reduced from 0.1, 1, 10, and 100 mM NaCl (Phases 1 and 2) to DI water (Phase 3) at q_w = 0.2 (Figure 3a) and 0.5 (Figure 3b) cm min^{-1}. A reduction in the solution IS to DI water initiated a rapid release pulse that decreased over time. This result has typically been attributed to elimination of the secondary minimum.[30,60,61] However, interaction energy calculations predict an insignificant influence of the secondary minimum on spore retention on a microscopically smooth surface (Table 1). Alternatively, some spores that interacted in a shallow primary minimum (due to Born repulsion and nanoscale roughness) may be released when the solution IS was

DOI: 10.1021/acs.est.5b05296
Environ. Sci. Technol. 2016, 50, 1295−1303

reduced to DI water.[41] Figure 3 also shows release behavior following a 12 h flow interruption and continued flushing of DI water at the same flow rate. The flow interruption caused a second release pulse that subsequently decreased with continued DI water flushing. This release pulse reflects the influence of slow microbe diffusion from microscopic roughness locations and/or finite primary minima.

Peak values of C/C_o in the transient release pulses in Figure 3 were sometimes very high and depended on the initial IS and flow rate during Phases 1 and 2 that controlled the amount of retention. In addition, peak values of C/C_o also depended on the reversibility of retained microbes. An improved understanding of the release behavior can be obtained by considering mass balance information shown in SI Table S1 and Table 2. In particular, the initial microbe mass on the solid phase after completion of Phases 1 and 2 (M_S) was determined as $M_S = 1 - M_{eff}$, and showed a systematic increase with IS (see the above section for a detailed explanation). Mass balance information for the release pulse before (M_{DI}) and after (M_{FI}) the flow interruption provides a conservative estimate of the maximum value of $F_{rev} = (M_{DI} + M_{FI})/M_S$ (Table 2). However, it should be acknowledged that the value of F_{rev} in eqs 1 and 2 may actually be smaller under steady-state flow and solution chemistry conditions. Note that $F_{irrev} = 1 - F_{rev}$ increased with solution IS and decreased with q_w (Table S1), and this indicates that a significant amount of spores interacted in a primary minimum that was not readily reversible. Primary minimum interactions may occur under unfavorable conditions as a result of nanoscale roughness and chemical heterogeneity.[49,50] Corresponding values of F_{rev} systematically increased with decreasing IS and increasing q_w (Table 2). The increase in F_{rev} with increasing q_w indicates that some of the primary minimum interactions were shallow (due to Born repulsion and nanoscale roughness) and subject to hydrodynamic and diffusive removal. The opposite dependency of M_s and F_{rev} on IS produced maximum amounts of release during Phase 3 at intermediate IS (1 and 10 mM) levels (Figure 3).

Kim et al.[30] also conducted a transient release experiment for oocysts in ultrapure quartz sand. Similar to Figure 3, this experiment was conducted by reducing the solution IS from 1 mM (Phases 1 and 2) to DI water (Phase 3), and included a 12 h flow interruption. Values of M_{DI} were quite similar for oocysts and spores (0.17 and 0.15, respectively), and M_{FI} was slightly larger for oocysts (0.26) than spores (0.20). This indicates that similar release processes were operative for both oocysts and spores. However, the value of F_{rev} was considerably larger for oocysts (0.58) than spores (0.42), and this suggests a greater potential for oocyst than spore release because of greater hydrodynamic forces (e.g., the drag force increases with the cube of the microbe radius). Kim et al.[30] did not measure transient oocyst release curves under the other physicochemical conditions in the ultrapure quartz sand. Hence, direct comparison of the amounts of spore and oocyst release for other physicochemical conditions was not possible. However, Kim et al.[30] did measure the transient release curves for oocysts in 710 μm Ottawa sand at IS levels of 0.1 and 100 mM when q_w equaled 0.2 and 0.5 cm min^{-1}. Similar to spores (Table 2), values of F_{rev} increased with q_w at both IS levels;for example, F_{rev} increased from 0.16 to 0.49 at IS = 0.1 and from 0.59 to 0.73 at IS = 100 mM when q_w increased from 0.2 to 0.5 cm min^{-1}. In contrast to spores (Table 2), the value of F_{rev} for oocysts actually increased with IS. Recall that Table 1 indicates that the depth of the primary minimum was shallower for oocysts at higher IS due to the presence of nanoscale roughness and Born repulsion, and this could also produce larger values of F_{rev} at higher IS.

■ ENVIRONMENTAL IMPLICATIONS

Variability of microbial size and surface properties with strain, origin, and age are expected to have a strong influence on environmental fate.[27] Consequently, additional research studies and modeling approaches are justified to fully assess whether aerobic spores will always serve as a conservative surrogate for *Cryptosporidium* oocyst behavior. Nevertheless, our results clearly demonstrate that *B. subtilis* spores served as a conservative surrogate for *C. parvum* oocyst transport and retention over a range of physicochemical conditions. However, low levels of spore and oocyst release were observed in breakthrough curves over a range of physicochemical conditions. Simulation results indicated that the long-term transport of oocysts at a particular setback distance will be strongly dependent on these release rates and the fraction of microbes that is reversibly retained (F_{rev}). Estimates of the maximum value of F_{rev} were obtained from transient release experiments in which the solution IS was reduced to DI water. Values of F_{rev} were quite large for both spores and oocysts, suggesting the need to consider release in assessing environmental fate. The value of F_{rev} increased with q_w for both spores and oocysts, whereas F_{rev} decreased with the initial IS (Phases 1 and 2) for spores and increased with the initial IS for oocysts. This different dependency of F_{rev} on the initial IS was attributed to differences in the microbe's zeta potentials and interaction energy profiles on a rough surface. In particular, the weak negative charge of oocysts produced shallower primary minima as the IS increased on a nanoscale rough surface, but this was not observed for the more negatively charged spores. Release results suggest that spores sometimes serve as a conservative indicator of oocyst release, but not always (such as at high IS = 100 mM).

■ ASSOCIATED CONTENT

Supporting Information

The Supporting Information is available free of charge on the ACS Publications website at DOI: 10.1021/acs.est.5b05296.

Details pertaining to (i) spore propagation and preparation (S1); (ii) oocyst preparation, analysis, and column experiments (S2); (iii) XDLVO calculations (S3); (iv) the derivation of the expression for the setback distance (S4); and (v) discussion of zeta potential information (S5). Figure S1 provides a plot of spore, oocyst, and quartz zeta potentials as a function of IS. Table S1 provides full mass balance information for the column experiments. Table S2 provides information on the fitted model parameters and their standard error (PDF)

■ AUTHOR INFORMATION

Corresponding Author

*Phone: (951) 369-4857; fax: (951)342-4964; e-mail: Email:Scott.Bradford@ars.usda.gov.

Notes

The authors declare no competing financial interest.

DOI: 10.1021/acs.est.5b05296
Environ. Sci. Technol. 2016, 50, 1295−1303

■ ACKNOWLEDGMENTS

This research was supported by the USDA, ARS, NP 214. We thank Philip Berger of the U.S. EPA for helpful comments and discussion concerning this manuscript.

■ REFERENCES

(1) Embrey, S. S.; Runkle, D. L. *Microbial Quality of the Nation'S Groundwater Resources, 1993−2004*; Sci. Investigations Rep. 2006−5290; U.S. Geological Survey: Reston, VA, 2006.
(2) WHO. *Guidelines for Drinking-Water Quality.*, 4th ed.; World Health Organization: Geneva, Switzerland, 2011.
(3) Prüss, A.; Kay, D.; Fewtrell, L.; Bartram, J. Estimating the burden of disease from water, sanitation, and hygiene at a global level. *Environ. Health Perspect.* **2002**, *110*, 537−542.
(4) Gleick, P. H. *Dirty-water: Estimated Deaths from Water-related Diseases 2000−2020*. Pacific Institute for Studies in Development, Environment, and Security, Oakland, CA, 2002.
(5) Bain, R.; Cronk, R.; Hossain, R.; Bonjour, S.; Onda, K.; Wright, J.; Yang, H.; Slaymaker, T.; Pruss-Ustun, A.; Bartram, J. Global assessment of exposure to faecal contamination through drinking water based on a systematic review. *Trop. Med. Int. Health* **2014**, *19*, 917−927.
(6) United States Environmental Protection Agency, *Surface water treatment rules: What do they mean to you?* EPA 816-R-11−009, 2011.
(7) United States Environmental Protection Agency. National primary drinking water regulations: Ground water rule. *Fed. Regist.* **2006**, *71*, 65574−65660.
(8) United States Environmental Protection Agency, *Long Term 2 Enhanced Surface Water Treatment Rule Toolbox Guidance Manual*. EPA 815-R-0-16, 2010.
(9) Robertson, L. J.; Gjerde, B. K. *Cryptosporidium* oocysts: challenging adversaries? *Trends Parasitol.* **2007**, *23*, 344−347.
(10) Tufenkji, N.; Dixon, D. R.; Considine, R.; Drummond, C. J. Multi-scale *Cryptosporidium*/sand interactions in water treatment. *Water Res.* **2006**, *40*, 3315−3331.
(11) MacKenzie, W. R.; Hoxie, N. J.; Proctor, M. E.; Gradus, M. S.; Blair, K. A.; Peterson, D. E.; Kazmierczak, J. J.; Addiss, D. G.; Fox, K. R.; Rose, J. B.; Davis, J. P. A massive outbreak in Milwaukee of *Cryptosporidium* infection transmitted through the public water supply. *N. Engl. J. Med.* **1994**, *331*, 161−167.
(12) Widerström, M.; Schönning, C.; Lilja, M.; Lebbad, M.; Ljung, T.; Allestam, G.; Ferm, M.; Bjorkholm, B.; Hansen, A.; Hitula, J.; Langmark, J.; Lofdahl, M.; Omberg, M.; Reuterwall, C.; Samuelsson, E.; Widgren, K.; Wallensten, A.; Lindh, J. Large outbreak of *Cryptosporidium hominis* infection transmitted through the public water supply, Sweden. *Emerging Infect. Dis.* **2014**, *20*, 581−589.
(13) Korich, D. G.; Mead, J. R.; Madore, M. S.; Sinclair, N. A.; Sterling, C. R. Effects of ozone, chlorine dioxide, chlorine, and monochloramine on *Cryptosporidium parvum* oocyst viability. *Appl. Environ. Microbiol.* **1990**, *56*, 1423−1428.
(14) Carmena, D.; Aguinagalde, X.; Zigorraga, C.; Fernández-Crespo, J. C.; Ocio, J. A. Presence of *Giardia* cysts and *Cryptosporidium* oocysts in drinking water supplies in northern Spain. *J. Appl. Microbiol.* **2007**, *102*, 619−629.
(15) Robertson, L. J.; Campbell, A. T.; Smith, H. V. Survival of *Cryptosporidium parvum* oocysts under various environmental pressures. *Appl. Environ. Microbiol.* **1992**, *58*, 3494−3500.
(16) Harris, J. R.; Petry, F. *Cryptosporidium parvum*: structural components of the oocyst wall. *J. Parasitol.* **1999**, *85*, 839−849.
(17) Hancock, C. M.; Rose, J. B.; Callahan, M. Crypto and *Giardia* in US ground water. *J. Am. Water Works Assn.* **1998**, *90*, 58−61.
(18) Ryan, U.; Hijjawi, N. New developments in *Cryptosporidium* research. *Int. J. Parasitol.* **2015**, *45*, 367−373.
(19) Clancy, J. L.; Gollnitz, W. D.; Tabib, Z. Commercial labs: how accurate are they? *J. Am. Water Works Assn.* **1994**, *86*, 89−97.
(20) Karanis, P.; Sotiriadou, I.; Kartashev, V.; Kourenti, C.; Tsvetkova, N.; Stojanova, K. Occurrence of *Giardia* and *Cryptosporidium* in water supplies of Russia and Bulgaria. *Environ. Res.* **2006**, *102*, 260−271.
(21) Brown, R. A.; Cornwell, D. A. Using spore removal to monitor plant performance for *Cryptosporidium* removal. *J. Am. Water Works Assn.* **2007**, *99*, 95−109.
(22) Allen, M. J.; Clancy, J. L.; Rice, E. W. The plain, hard truth about pathogen monitoring. *J. Am. Water Works Assn.* **2000**, *92*, 64−76.
(23) Nicholson, W. L.; Munakata, N.; Horneck, G.; Melosh, H. J.; Setlow, P. Resistance of *Bacillus* endospores to extreme terrestrial and extraterrestrial environments. *Microbiol. Mol. Biol. Rev.* **2000**, *64*, 548−572.
(24) Rice, E. W.; Fox, K. R.; Miltner, R. J.; Lytle, D. A.; Johnson, J. H. A microbiological surrogate for evaluating treatment efficiency. In *Proc. Am. Water Works Assn. Water Quality Technology Conference*, San Francisco, CA, **1994**.
(25) Galofr, B.; Israel, S.; Dellund, J.; Ribas, F. Aerobic bacterial spores as process indicators for protozoa cysts in water treatment plants. *Water Sci. Technol.* **2004**, *50*, 165−172.
(26) Mazoua, S.; Chauveheid, E. Aerobic spore-forming bacteria for assessing quality of drinking water produced from surface water. *Water Res.* **2005**, *39*, 5186−5198.
(27) Headd, B.; Bradford, S. A. Use of aerobic spores as a surrogate for *Cryptosporidium* oocysts in surface water and groundwater. *Water Res.* **2016**, *90*, 185−202.
(28) Kennedy, M. J.; Reader, S. L.; Swierczynski, L. M. Preservation records of micro-organisms: evidence of the tenacity of life. *Microbiology* **1994**, *140*, 2513−2529.
(29) Abbaszadegan, M.; Rauch-Williams, T.; Johnson, W. P.; Hubbs, S. A. *Methods to assess GWUDI and bank filtration performance*; Water Research Foundation, Denver, CO, 2011.
(30) Kim, H. N.; Walker, S. L.; Bradford, S. A. Coupled factors influencing the transport and retention of *Cryptosporidium parvum* oocysts in saturated porous media. *Water Res.* **2010**, *44*, 1213−1223.
(31) Bradford, S. A.; Torkzaban, S.; Leij, F.; Simunek, J. Equilibrium and kinetic models for colloid release under transient solution chemistry conditions. *J. Contam. Hydrol.* **2015**, *181*, 141−152.
(32) Kim, H. N.; Bradford, S. A.; Walker, S. L. *Escherichia coli* O157:H7 transport in saturated porous media: Role of solution chemistry and surface macromolecules. *Environ. Sci. Technol.* **2009**, *43*, 4340−4347.
(33) Ahimou, F.; Paquot, M.; Jacques, P.; Thonart, P.; Rouxhet, P. G. Influence of electrical properties on the evaluation of the surface hydrophobicity of Bacillus subtilis. *J. Microbiol. Methods* **2001**, *45*, 119−126.
(34) Derjaguin, B. V.; Landau, L. D. Theory of the stability of strongly charged lyophobic sols and of the adhesion of strongly charged particles in solutions of electrolytes. *Prog. Surf. Sci.* **1993**, *43*, 30−59.
(35) Verwey, E. J. W.; Overbeek, J. Th. G. *Theory of the Stability of Lyophobic Colloids*; Elsevier: Amsterdam, 1948.
(36) Hogg, R.; Healy, T. W.; Fuerstenau, D. W. Mutual coagulation of colloidal dispersions. *Trans. Faraday Soc.* **1966**, *62*, 1638−1651.
(37) Elimelech, M.; Gregory, J.; Jia, X.; Williams, R. A. *Particle Deposition and Aggregation: Measurement, Modeling, And Simulation*; Butterworth-Heinemann: Oxford, England, 1995.
(38) Gregory, J. Approximate expression for retarded van der Waals interaction. *J. Colloid Interface Sci.* **1981**, *83*, 138−145.
(39) Kuznar, Z. A.; Elimelech, M. *Cryptosporidium* oocyst surface macromolecules significantly hinder oocyst attachment. *Environ. Sci. Technol.* **2006**, *40*, 1837−1842.
(40) Ruckenstein, E.; Prieve, D. C. Adsorption and desorption of particles and their chromatographic separation. *AIChE J.* **1976**, *22*, 276−285.
(41) Torkzaban, S.; Bradford, S. A. Critical role of surface roughness on colloid retention and release in porous media. *Water Res.* **2016**, *88*, 274−284.

DOI: 10.1021/acs.est.5b05296
Environ. Sci. Technol. 2016, 50, 1295−1303

(42) Šimůnek, J.; van Genuchten, M. T.; Šejna, M. Development and applications of the HYDRUS and STANMOD software packages and related codes. *Vadose Zone J.* **2008**, *7*, 587−600.
(43) Shen, C.; Lazouskaya, V.; Jin, Y.; Li, B.; Ma, Z.; Zheng, W.; Huang, Y. Coupled factors influencing detachment of nano- and micro-sized particles from primary minima. *J. Contam. Hydrol.* **2012**, *134*−*135*, 1−11.
(44) Bradford, S. A.; Torkzaban, S. Colloid interaction energies for physically and chemically heterogeneous porous media. *Langmuir* **2013**, *29*, 3668−3676.
(45) Bradford, S. A.; Torkzaban, S. Determining parameters and mechanisms of colloid retention and release in porous media. *Langmuir* **2015**, *31*, 12096−12105.
(46) Considine, R. F.; Dixon, D. R.; Drummond, C. J. Laterally-resolved force microscopy of biological microspheres oocysts of *Cryptosporidium parvum*. *Langmuir* **2000**, *16*, 1323−1330.
(47) Kuznar, Z. A.; Elimelech, M. Adhesion kinetics of viable *Cryptosporidium parvum* oocysts to quartz surfaces. *Environ. Sci. Technol.* **2004**, *38*, 6839−6845.
(48) Kuznar, Z. A.; Elimelech, M. Role of surface proteins in the deposition kinetics of *Cryptosporidium parvum* oocysts. *Langmuir* **2005**, *21*, 710−716.
(49) Bendersky, M.; Davis, J. M. DLVO interaction of colloidal particles with topographically and chemically heterogeneous surfaces. *J. Colloid Interface Sci.* **2011**, *353*, 87−97.
(50) Duffadar, R. D.; Davis, J. M. Dynamic adhesion behavior of micrometer-scale particles flowing over patchy surfaces with nanoscale electrostatic heterogeneity. *J. Colloid Interface Sci.* **2008**, *326*, 18−27.
(51) Burdick, G. M.; Berman, N. S.; Beaudoin, S. P. Hydrodynamic particle removal from surfaces. *Thin Solid Films* **2005**, *488*, 116−123.
(52) Bradford, S. A.; Torkzaban, S.; Shapiro, A. A theoretical analysis of colloid attachment and straining in chemically heterogeneous porous media. *Langmuir* **2013**, *29*, 6944−6952.
(53) Tufenkji, N.; Miller, G. F.; Ryan, J. N.; Harvey, R. W.; Elimelech, M. Transport of *Cryptosporidium* oocysts in porous media: Role of straining and physicochemical filtration. *Environ. Sci. Technol.* **2004**, *38*, 5932−5938.
(54) Hijnen, W. A.; Dullemont, Y. J.; Schijven, J. F.; Hanzens-Brouwer, A. J.; Rosielle, M.; Medema, G. 2007. Removal and fate of *Cryptosporidium parvum*, *Clostridium perfringens* and small-sized centric diatoms (*Stephanodiscus hantzschii*) in slow sand filters. *Water Res.* **2007**, *41*, 2151−2162.
(55) Bradford, S. A.; Bettahar, M. Straining, attachment, and detachment of oocysts in saturated porous media. *J. Environ. Qual.* **2005**, *34*, 469−478.
(56) Yao, K.-M.; Habibian, M. T.; O'Melia, C. R. Water and waste water filtration: Concepts and applications. *Environ. Sci. Technol.* **1971**, *5*, 1105−1112.
(57) Tufenkji, N.; Elimelech, M. Correlation equation for predicting single-collector efficiency in physicochemical filtration in saturated porous media. *Environ. Sci. Technol.* **2004**, *38*, 529−536.
(58) Harter, T.; Wagner, S.; Atwill, E. R. Colloid transport and filtration of *Cryptosporidium parvum* in sandy soils and aquifer sediments. *Environ. Sci. Technol.* **2000**, *34*, 62−70.
(59) Cortis, A.; Harter, T.; Hou, L.; Atwill, E. R.; Packman, A. I.; Green, P. G. Transport of *Cryptosporidium parvum* in porous media: Long-term elution experiments and continuous time random walk filtration modeling. *Water Resour. Res.* **2006**, *42*, W12S13.
(60) Tufenkji, N.; Elimelech, M. Spatial distributions of *Cryptosporidium* oocysts in porous media: Evidence for dual mode deposition. *Environ. Sci. Technol.* **2005**, *39*, 3620−3629.
(61) Tufenkji, N.; Elimelech, M. Breakdown of colloid filtration theory: Role of the secondary energy minimum and surface charge heterogeneities. *Langmuir* **2005**, *21*, 841−852.

DOI: 10.1021/acs.est.5b05296
Environ. Sci. Technol. 2016, 50, 1295−1303